Batteries 2020 – Lithium-ion battery first and second life ageing, validated battery models, lifetime modelling and ageing assessment of thermal parameters

Timmermans, Jean-Marc Paul; Nikolian, Alexandros; De Hoog, Joris; Gopalakrishnan, Rahul; Goutam, Shovon; Omar, Noshin; Coosemans, Thierry Clement; Van Mierlo, Joeri

Published in:
EPE 2016 Conference Proceedings

Publication date:
2016

Document Version:
Submitted manuscript

Batteries 2020 – Lithium-ion battery first and second life ageing, validated battery models, lifetime modelling and ageing assessment of thermal parameters

Timmermans, Jean-Marc; Nikolian, Alexandros; De Hoog, Joris; Gopalakrishnan, Rahul; Goutam, Shovon; Omar, Noshin; Coosemans, Thierry; Van Mierlo, Joeri.
VRIJE UNIVERSITEIT BRUSSEL, MOBI Research Group
Pleinlaan 2
Brussels, Belgium
Tel.: +32 / (2) – 629.38.07.
Fax: +32 / (2) – 629.36.20.
E-Mail: Jean-Marc.Timmermans@vub.ac.be
URL: mobi.vub.ac.be

Warnecke, Alexander; Uwe Sauer, Dirk.
RWTH Aachen University, ISEA,
Chair for Electrochemical Energy Conversion and
Storage Systems,
Aachen, Germany
E-Mail: batteries@isea.rwth-aachen.de
URL: isea.rwth-aachen.de

Swierczynski, Maciej; Stroe, Daniel Ioan.
Aalborg University, Department of Energy Technology
URL: et.aau.dk

Martinez-Laserna, Egoitz; Sarasketa-Zabala, Elixabet; Gastelurrutia, Jon; Nieto Nerea.
IK4-IKERLAN
Alava, Spain

Acknowledgements

The authors thank all partners in the BATTERIES2020 project for their contributions to the results presented in this paper and for their excellent cooperation. This work is funded by the European Union through the NMP.2013-1 Batteries2020 project (Grant agreement GC.NMP.2013-1 / GA nº 608936). Further, the Vrije Universiteit Brussel acknowledges the "Flanders Make" for the support to our team.

Keywords

Batteries, Energy Storage, Simulation, Modelling, Electric vehicle.

Abstract

The European Project “Batteries 2020” unites nine partners jointly working on research and the development of competitive European automotive batteries. The project aims at increasing both the energy density and lifetime of large format pouch lithium-ion batteries towards the goals targeted for automotive batteries (250 Wh/kg at cell level, over 4000 cycles at 80% depth of discharge). Three parallel strategies are followed in order to achieve those targets: (i) Highly focused materials development; two improved generations of NMC cathode materials allows to improve the performance, stability and cyclability of state of the art battery cells. (ii) Better understanding of the

ageing phenomena; a robust and realistic testing methodology has been developed and was carried out. Combined accelerated, real driving cycle tests, real field data, post-mortem analysis, modelling and validation with real driving profiles was used to obtain a thorough understanding of the degradation processes occurring in the battery cells. (iii) Reduction of battery cost; a way to reduce costs, increase battery residual value and improve sustainability is to consider second life uses of batteries used in electric vehicle application. These batteries are still operational and suitable to less restrictive conditions, such as those for stationary and renewable energy application. Therefore, possible second life opportunities have been identified and further assessed. In this paper, the main ageing effects of lithium ion batteries are explained. Next, an overview of different validated battery models will be discussed. Finally, a methodology for assessing the performance of the battery cells in a second life application is presented.

Introduction

The Batteries 2020 project is structured in nine separate work packages and the work plan is designed towards efficient achievement of significant results (see Figure 1). A reference first generation (G1) battery cell is being used at the beginning of the project as a benchmark for a better and thorough ageing understanding, development of standard methodology, modelling and lifetime prediction validation. In parallel, advanced active materials have been developed towards an intermediate second generation (G2) of improved high-energy cells, that are good performing and age robust. These novel G2 cells have been characterized by the optimized test protocols and procedures developed while analysing the G1 cells. In parallel to G2 cells ageing, second life uses of G1 cells was assessed and further improved materials for the third generation (G3) cells, towards EV targets has been further developed. The project is thought in terms of efficient iteration loops promoting rapid generation of results and know-how that can be implemented into the new generation of active materials, battery cells, testing methodologies and test procedures.

Through the achievement of the different tasks, the project will deliver the knowledge for competitive European cell production. Standardized and optimized methods for lifetime testing and a lifetime model has been developed. A thorough understanding of ageing and cell degradation has been achieved through combination of tests, models and prediction. A complete characterization of the cells has been carried out and was used as the basis for the development of an electrical, an electrochemical, a thermal and a lifetime model. Further, the effect of variability of the first life aged cells on second life use was also analysed, which allow assessing the possible cost reduction of automotive batteries due to the identification of the residual value. The methodology employed for such second life battery ageing analysis is described in the last section of the present paper.

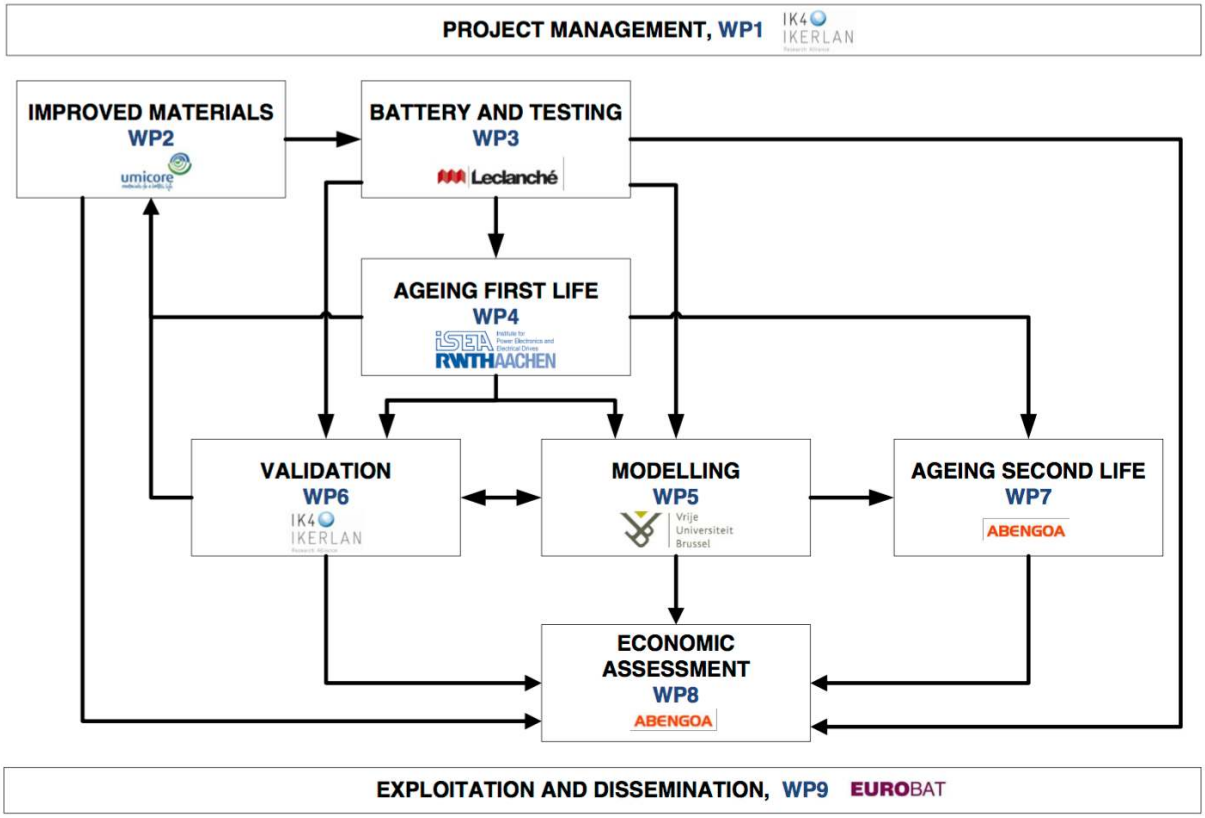

Fig.1: work plan of the Batteries 2020 project.

Lithium ion batteries ageing effects

2016 the lithium-ion battery is commercially available for 25 years and has improved since the market entrance drastically. This shows that a lot of effort was put into research finding new materials for longer lifetime, higher energy density and power capability. Since the field of application has changed in these 25 years from consumer electronics and handheld devices to a main component of the drive train of electric vehicles, the lifetime comes more into focus. Depending of the application goals for service life differ drastically. Most challengeable and driving at the moment are mobile automotive applications. As explained in the abstract the goal of the project was to develop a battery that stands over 4000 cycles at 80% depth of discharge, which would result in a total drivable range from 400,000 km (100 km range) to 2,000,000 km (500 km range). But beside the total range a car can cover, also the stored (idle) time is very important. The typical usage of a vehicle in Europe is between 8-10 years. This show that lifetime just in storage is also a challenging task.

To achieve this we have to take a look at this very complex system of many components. Anode, cathode, separator and electrolyte interact while charged and discharged and during storage. This makes the ageing even a more complex process, where it is not possible to separate different ageing mechanisms. But it is possible to determine the most dominant ageing processes for the components of the cells, and is shortly discussed below.

The anode is the best known component in lithium ion batteries and consists in most cases of carbon materials, like graphite or hard carbon. For these materials the dominant ageing effects are basically known and can be separated in three parts:

- Surface film formation on the particles
- Degradation of the active material
- Lithium metal deposition on the anode surface

These materials have a typical voltage level of 0.05-0.5 V against metallic lithium when charged and discharged. At this potential the commonly used electrolytes (carbonates) are not stable and decompose on the anode surface within the first charge. The formed layer is called solid electrolyte interphase (SEI) and is necessary for the function of the battery. If this layer is formed well, it prevents a further decomposition of the electrolyte on the anode surface. Within this process mobile lithium between the electrodes is involved and also integrated into the SEI. Loss of mobile lithium leads to a capacity fade. Unfortunately the SEI doesn't stop after the first cycle, but continues over the whole lifetime, which makes it the most dominant ageing effect in a lithium ion battery.

Beside the film formation the graphitic anode materials also undergoes a volume change of 10% in the intercalation and deintercalation process of lithium. Volume change in active materials is equivalent to mechanical stress inside the particle and the SEI and results in cracks. Loss of active lithium by new SEI formation and loss of active material by contact loss are the consequences. Additionally a thicker surface layer on the anode results also in an impedance rise which is equivalent to power fade of the battery.

As mentioned above the third main ageing mechanism at the anode side of a lithium ion battery is lithium metal deposition, which is also known as "plating". Within the process of lithium plating, the intercalation reaction at the anode is too slow and the potential to low, so that the lithium ions tend to deposit on the particles in the metallic form. The low intercalation rate and the low potential at the anode (or parts of the anode) can be caused by low temperatures, high charging currents and inhomogeneous current and potential distributions. Deposited lithium reacts directly with the electrolyte and also forms a layer at the metallic surface. This consumes active lithium and electrolyte which results in capacity and power loss. Beside the influence on the battery performance, lithium has also the tendency to grow in dendritic form, which is a safety risk because these dendrites could grow and result in a shortcut between the electrodes.

The focus in this project is on the development of new and better cathode materials. The ageing effects at the cathode, and especially the new materials, are less known, but can also be summarized within three groups of effects:

- Ageing of the active material
- Surface film formation
- Interaction of ageing products with the negative electrode

The active materials of the cathode in nowadays electric vehicles and also in this project are layered metal oxides with a variation of the used metals. The changes of these materials and the influence on the capacity loss are very small compared to the capacity loss over the lifetime. Similar to the anode mechanical stress can cause loss of active material and change of the composition can change the lattice structure of the crystals, which both lead to capacity loss and an increase in impedance. Similar to the anode, the stability of the electrolytes influences the surface film formation on the cathode side. Increasing the voltage of the electrode above 4.5 V against metallic lithium, the electrolyte gets decomposed on the cathode. This film formation also plays just a minor role for the total ageing of the cell, since tis high potentials are avoided by the upper cut-off voltage of the cell. Some materials, like manganese spinel or manganese rich nickel-manganese-cobalt layered oxides (NMC), the dissolution of the transition metal manganese plays the major role in the interaction of the anode. The manganese ions migrate to the anode and destroy the SEI layer, which leads in new SEI formation and with this an accelerated capacity loss and impedance increase.

All the described ageing effects occur at the same time, but have different accelerators and rates. State of the art for identification of the influencing factors is based on accelerated ageing tests. These tests are performed with a variation of operating conditions like temperature, current rate, depth of discharge (DoD) and state of charge (SoC). The acceleration in comparison to the application is realized by deleting pauses and rest times. For studying the ageing mechanisms at storage conditions the cells are stored under defined and controlled environmental conditions and capacity fade and

impedance increase are monitored. To get a good overview, a high number of cells need to be tested and each operating condition needs to be represented by multiple cells.

In the Project “Batteries2020” the first generation of cells was tested with 161 batteries at 47 different conditions. In figure 2 you can see the calendric ageing behaviour of the commercial cell which is (in most of its behaviour) representative for many different cells. The capacity loss is faster for cells at higher temperatures, this indicates that cells should not be stored at high temperatures when not used. Additionally we can see in the middle of figure 2 that higher values for the SoC leads to much faster capacity degradation. A result from these ageing curves is that for an example an electric vehicle should best not be parked or stored for a long time at a high state of charge and only be charged just before the use, to achieve maximum battery life. These ageing curves are also used to parameterize the models, which are described in the next section.

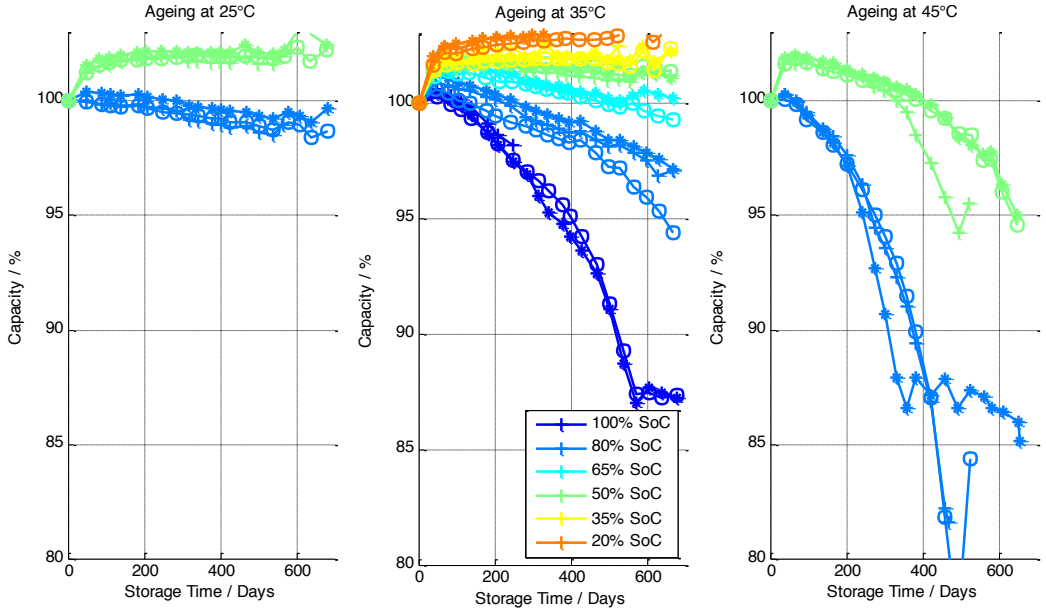

Fig. 2: Calendric ageing curves from the G1 “Batteries2020”cell at different temperatures and SoC.

As described above, beside the pure storage of the cell, the use (cycling) of the battery also adds, additional capacity loss. Figure 3 shows the remaining capacity curves of cycled cells where the cell temperature was kept 25°C while cycling. Also here the cycling depth (DoD) has a big influence on the lifetime. Cells that were charged and discharged completely in every cycle are ageing much faster than cells that were only discharged partially. As a conclusion we can say that discharging the cell more deeply before recharging, is not beneficial for the lifetime. Keeping in mind the findings from calendric ageing, long time storage at high SOC levels is not beneficial for the battery ageing. Further information on the ageing and the internal processes can be found in our publications that will be published in the near future.

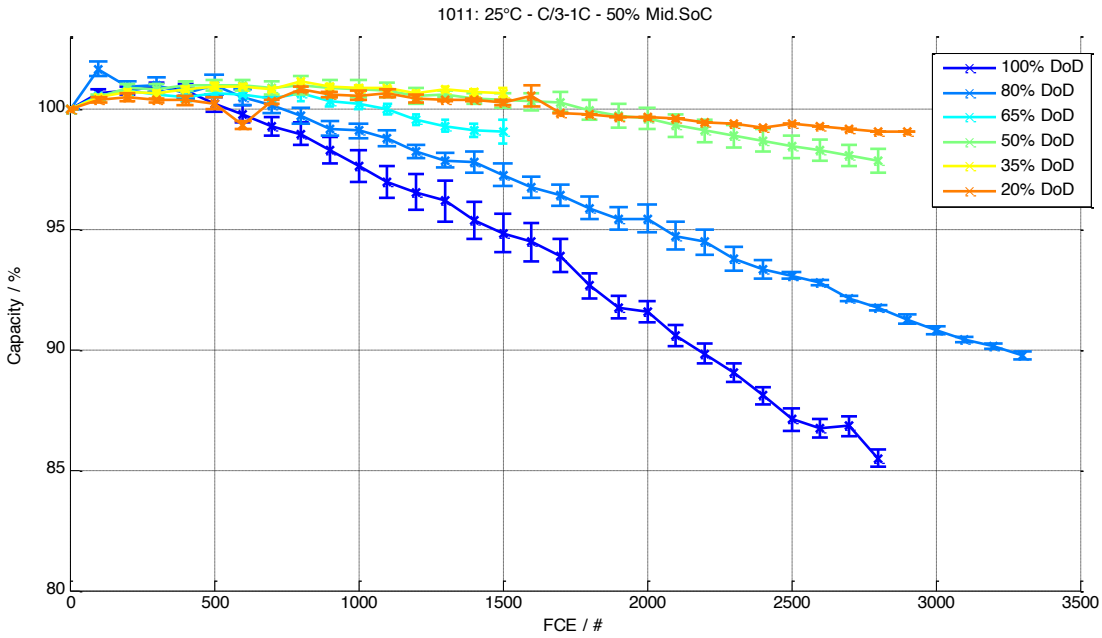

Fig. 3: Remaining capacity curves of cyclic aged cell at 25°C for different values of the depth of discharge (DoD). FEC denotes full equivalent cycles and provides a same Ah-throughput value for the different depth-of-discharge conditions.

Validated dynamic electrical battery model

Models that describe the electrical behaviour of the battery have been extensively studied and developed in academia [1]–[9]. There exist multiple models that can be used to describe the electrical response of the battery and in this study those have been categorized as follows:

- Analytical models;
- Electrical ECM models;
- Frequency domain models.

Electrical models are mainly semi-empirical models where characterization techniques are performed to identify the different parameters of the battery. Those characterization techniques have been extensively described in different standardization documents [6], [7], [10]–[13] and they are generally composed of:

- Capacity test: defining the discharge/charge capacity of the battery;
- Open circuit voltage (OCV) versus SoC test: relating the SoC levels with the open circuit voltage of the battery;
- Hybrid pulse power characterization (HPPC) test: to define the internal resistances and SoC of the battery;
- Electrochemical impedance spectroscopy (EIS) test: define the internal resistance and impedance of the battery.

Equivalent Circuit Model for NMC lithium-ion battery cells

A set of ECM models has been created to simulate the behaviour of the battery cell under different ECM topologies and temperatures conditions of the battery NMC chemistry of the Batteries 2020 project. In addition, different SoC-estimation techniques (Coulomb counting and extended Kalman Filter) have been incorporated into the electrical battery models.

The battery models created are based on parameters calculated from two types of characterization tests: the so-called normal and advanced characterisation tests. Normal and advanced characterization tests have been developed to acquire a better understanding of the battery cell behaviour at the complete rang of (from high to low) SoC levels. The normal characterization tests consists of performing a specific test (*i.e.*, HPPC, OCV-SoC) at each 5% step of the total SoC window, while advanced characterization tests consists of separating the total SoC window into three parts where the high SoC levels (from 100% to 90%) and the low SoC levels (from 10% to 0%) tests are performed in 2% steps of the SoC, while the middle SoC window (from 90% to 10%) with 5% steps. Two types of ECM topologies were utilized: the 1st order and the 2nd order Thévenin battery model. The extended Kalman filtering technique was applied on this 2nd order Thévenin battery model. Further, this topology that has also been validated with a more dynamic profile based on the Worldwide Harmonized Light vehicle (WLTC) driving profile. The validation of all models has been performed at multiple values of the temperature (from 15 °C, 25 °C, 35 °C and 45 °C) by means of the dynamic discharge pulse test (DDPT). The voltage response error between the simulated and measured results is calculated according to the Equation 1 below.

$$\text{err}\,\% = 100\times\frac{V_{\text{measured}} - V_{\text{simulated}}}{V_{\text{measured}}} \tag{1}$$

Table I: Results of the 1st Order Thevenin ECM models at different temperatures with normal characterization parameters in which the error remains lower than the proposed in the given specific SoC-window.

Temperature	SoC window	≤Error
15 °C	100%–16%	±2%
25 °C	100%–10%	±2%
35 °C	100%–12%	±2%
45 °C	100%–5%	±2%

Table II: Results of the 1st Order Thevenin ECM models at different temperatures with advanced charracterization parameters in which the error remains lower than the proposed ±2% in the given specific SoC-window.

Temperature	SoC window	≤Error
15 °C	100%–15%	±2%
25 °C	100%–7%	±2%
35 °C	100%–8%	±2%
45 °C	100%–4%	±2%

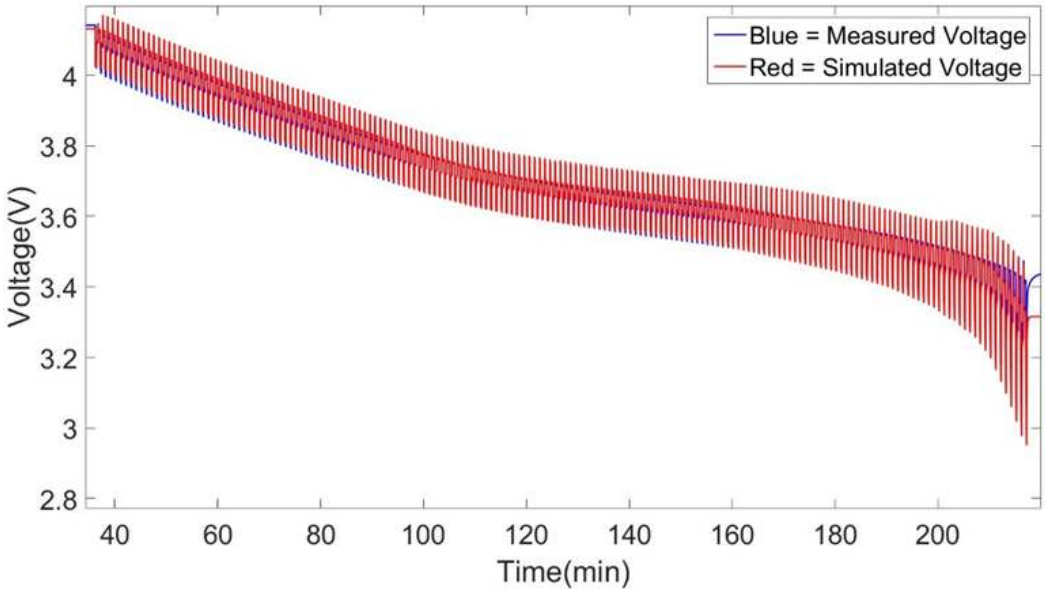

Fig. 4: Comparison of the 2nd order Thévenin ECM model simulated voltage response (red) with the measured voltage response (blue) based on the DDP test at 25 °C with Coulomb counting SoC estimation and with advanced characterization parameters.

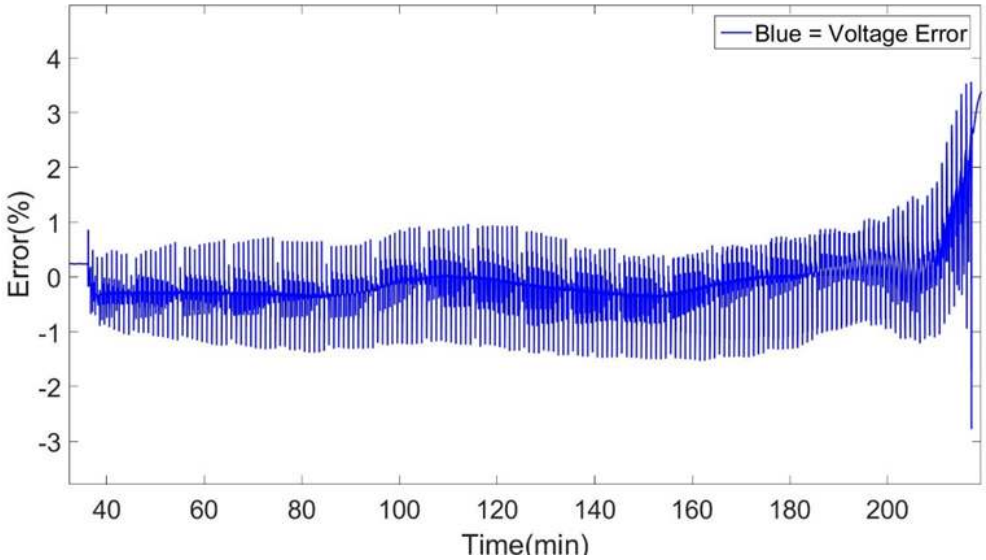

Fig. 5: Error of the 2nd order Thévenin ECM model based on the DDP test at 25 °C with Coulomb counting SoC estimation and with advanced characterization parameters.

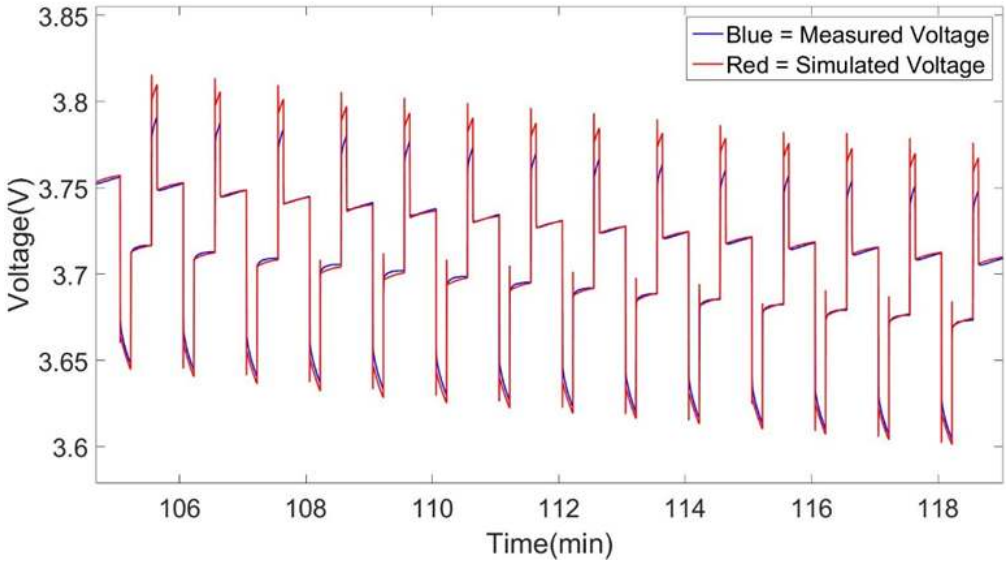

Fig. 6: Comparison of the dynamic behaviour of the 2nd order Thévenin ECM model simulated voltage response (red) with the measured voltage response (blue) based on the DDP test at 25 °C with Coulomb counting SoC estimation and with advanced characterization parameters.

Table III: Results of the 2nd Order Thévenin ECM models at different temperatures with advanced characterization parameters in which the error remains lower than the proposed error in the given specific SoC-window.

Temperature	SoC-window	≤Error
15 °C	100%–9%	±2%
25 °C	100%–7%	±2%
35 °C	100%–10%	±1%
45 °C	100%–4%	±1%

Table IV: Results of the 2nd Order Thévenin models at different temperatures with advanced characterization parameters & extended Kalman filter in which the error remains lower than the proposed error in the given specific SoC-window.

Temperature	SoC-window	≤Error
15 °C	100%–5%	±2%
25 °C	100%–0%	±2%
35 °C	100%–3%	±1%
45 °C	100%–0%	±1%

Observing these modelling results, some general observations can be mentioned:

- Higher temperature conditions leads to more efficient NMC lithium ion ECM modelling results;
- More complex ECM topologies (second order vs. first order ECM) will increase the accuracy of NMC lithium-ion ECM models;
- Applying a more advanced SoC estimation technique (Extended Kalman Filter vs. Coulomb counting) will increase the accuracy of NMC lithium-ion ECM models;
- The models created, can deal with dynamic profiles such as the WLTC profile.

The main conditions that are predominantly affecting the accuracy of the models is the temperature and the state of charge. This effect can be observed on both ECM topologies, for both types of characterization results used and for both the Coulomb counting and the extended Kalman filtering SoC estimation technique. This phenomenon can be explained by the fact that when operating a battery cell at higher temperatures, the kinetic electrochemical reactions inside the cell are improved, making the behaviour of the cell at this condition more pronounced and homogeneous compared to that at lower temperatures. Operating the cell at low SoC levels (typically below 10% SoC) at any temperature also results in a more unpredictable (nonlinear) manner. Thus, when determining the model parameters from the characterisation tests at low temperature and/or low SoC values, the resulting electrical ECM model will suffer from more non-linear errors during the simulation. The main errors that have been encountered during the simulations can be identified at the high and low SoC window of the simulations. This effect as described above is minimized when increasing the temperature condition at which the model parameters were created. Further, a clear improvement is observed in the models when changing the topology of the models from 1st to 2nd order Thévenin model. This effect can be clearly observed between the 1st and 2nd order Thévenin model at 25 °C models while also at the others temperatures. The 1st order Thévenin model at 25 °C using advanced characterization datasets has a similar overall accuracy as the 2nd order Thévenin model at 25 °C using advanced characterization datasets. However, the error at very high and low SoC-levels in the case of the 2nd order Thévenin model is further reduced.

Inspecting the 2nd order Thévenin models with Coulomb-counting and extended Kalman filtering SoC-estimation technique we observe a clear improvement in the accuracy of the model. Due to the extended Kalman filtering method, used to recalculate and actualize the SoC-value of the cell in the model, the overall accuracy of our models is further increased while we observed a clear improvement in the dynamic representations of the models. Comparing the 1st order models created with normal characterization and advance characterization datasets we observed that the accuracy of the models is increased but is not substantial as it is when changing temperature, topologies and SoC-estimation techniques. Furthermore, the dynamic behaviour has been improved more than the overall accuracy of these models by the change of the characterization datasets from normal to advanced.

Collecting all these observations the electrical model that should provide the best simulation accuracy and dynamic behaviours during the simulation should be models with complex topologies. In this regard, the most efficient model created for this study was the 2nd order Thévenin model with advanced characterization datasets and extended Kalman filtering SoC-estimation technique. The best performance is achieved when considering higher operating temperatures, in particular in when the cell is operated at 45 °C. Future work will investigate more in-depth the development of ECM models based on a high number of cells creating average parameters for a batch of cells and comparing them to average validations profiles provided by the combination of the validations results (average DDP and WLTC profiles for a batch of cells). This analysis will provide a better understanding of the behaviour of a set of NMC cells, which represents with higher fidelity the situation observed in an automotive battery pack combined with a BMS.

Development of a lifetime model

The aim of a lifetime model is to estimate the evolution of one or more performance parameters during the lifetime of the cell. For the "Batteries2020" project, these performance parameters are the following:

- Capacity
- Power capability

The capacity evolution is straightforward: it describes the total available charge or discharge capacity while the battery is subjected to various operating conditions (stress conditions), and thus degrading. The power capability evolution describes the capability of the cell to deliver power over the course of the lifetime of the cell, and this parameter is directly related to the internal resistance (RINT) of the cell.
Cell degradation happens both during operation (Cycling ageing) and during stationary time periods (Calendar Ageing), when no current is flowing through the cell. These are two independent factors in the degradation of the cell, and must be modelled independently.
The stress conditions are the external parameters that influence the cell performance degradation. These conditions are classified as follows:

- Cycling ageing stress factors:
- Temperature;
- Depth-of-Discharge (DOD);
- Middle State-of-Charge (Mid-SOC);
- Charge current rate;
- Discharge current rate.
- Calendar ageing stress factors:
- Storage Temperature
- Storage State-of-Charge

All these stress factors are independently influencing the degradation of the cell, and their influence must, therefore, be modelled separately. It is important to note that while the cell is subjected to cycling, calendar ageing will still take place.
Finally, the lifetime model must be able to estimate the capacity loss and power fade of a cell that is subjected to a driving profile, which means that both models (cycling ageing model and calendar ageing model) have to be able to work together in order to correctly estimate the ageing factor.

Cycling ageing modeling Input data

An important factor to take into account when developing a cycling ageing model is that while the cell is cycling, it's also subjected to calendar ageing. This is especially important since the aim of the combined ageing model is to estimate the ageing during cycling and calendar ageing combined. If we fail to account for the calendar ageing contribution to the overall cycling ageing data, the model will effectively estimate the calendar ageing twice**.**
This is effectively achieved in the following manner:

- Extract the dates of each capacity check-up test;
- Calculate the ageing contribution from ageing using the Calendar Ageing model;
- Subtract the capacity loss due to calendar ageing from the measured capacity values from the capacity tests.

The resulting capacity values can be considered to be the result of 'pure' cycling ageing. An example can be seen in Figure 7.

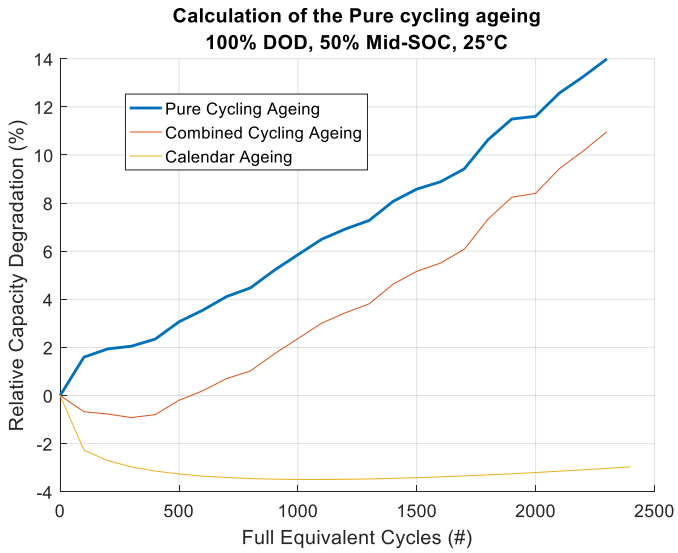

Fig. 7: Calculation of the pure cycling ageing.

Cycling ageing model

The following cycling stress factors are considered in this model[1]:

- Temperature (°C)
- Depth of Discharge (DOD, %)
- Middle State-of-Charge (Mid-SOC, %)

The general layout of the cycling ageing model can be found in Figure 8. As can be seen, the model currently consist of two stages, which are used in a sequential manner:

- Stage 1: Calculate the influence of the temperature and DOD, with following assumed conditions:
  - Mid-SOC: 50%;
  - Charge rate: C/3
  - Discharge rate: 1C
- Stage 2: Calculate the deviation in Capacity loss due to a Mid-SOC other than 50%.
- Final result: Add the results from Stage 1 and 2, resulting in the Capacity loss due to DOD, Mid-SOC, Temperature and Cycle number.

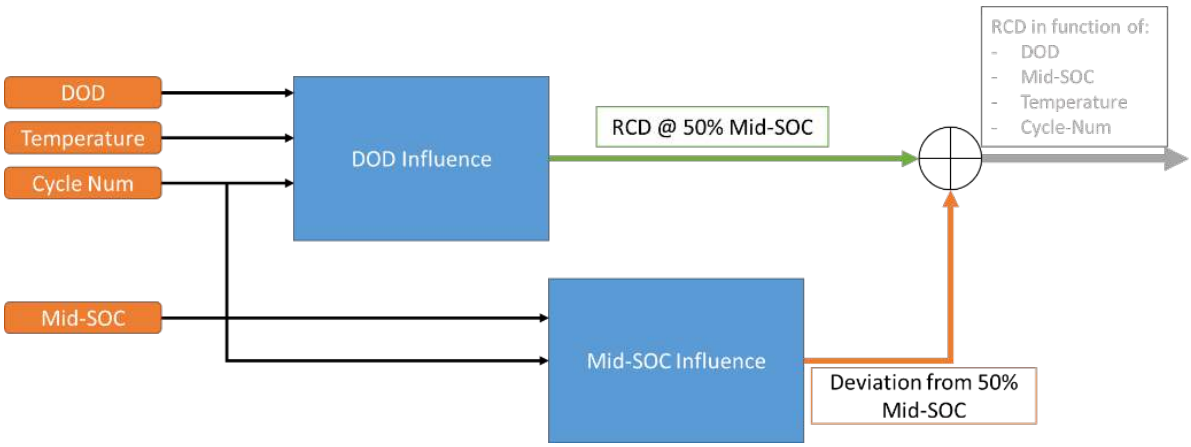

Fig. 8: General layout of the Batteries2020 Cycle Ageing model

[1] At the time of writing this paper, the influence of charge and discharge current rates has not been modeled yet, however, this is under development.

The model itself is constructed in two successive actions:

1. Extend the measured input data using a 2D polynomial
2. Use the extended input vectors as input for a 3D polynomial surface fit.

These two steps are visualized in Figures 9 and 10.

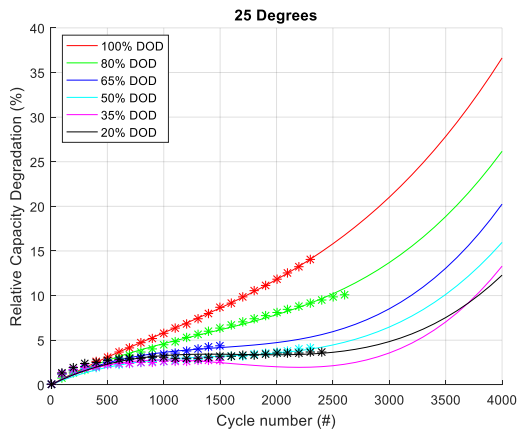

Fig. 9: 2D Extrapolation of measured input data

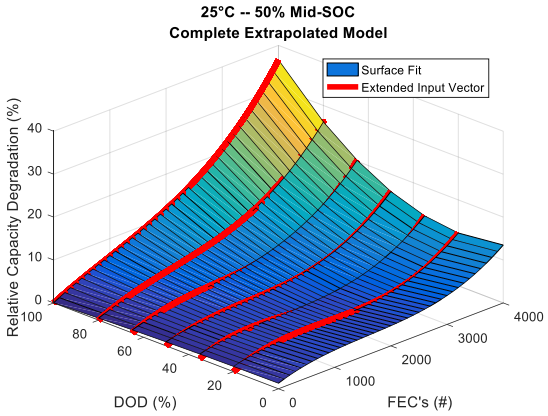

Fig. 10: 3D Surface fitting of extended input data

The final 3D Surface allows the interpolation between measured DOD levels, as well as extrapolation towards the EOL of the cell. As these surfaces are constructed for 3 input temperatures (25, 35 and 45°C), these are also used for interpolation between temperatures. The exact same methodology is used for fitting and modeling the influence of the Mid-SOC.

Calendar ageing model

The following calendar ageing stress factors are considered in the calendar-ageing model:

- Storage temperature (°C);
- Storage State-Of-Charge (%).

As the influence of these parameters are often quite hard to predict due to the fact that the time needed to perform tests that show sufficient calendar ageing is in most cases prohibitively long, the predictions are supported by two electrochemical equations:

1. Arrhenius equation, describing the evolution of the reaction rate depending on the temperature

$$A(T) = a * [exp(b/T)] \qquad (2)$$

2. Tafel equation, which relates the rate of an electrochemical reaction to the over-potential

$$\Delta V = A * ln(\frac{i}{i0}) \qquad (3)$$

The following empirical equation was found to fit the input measurement points:

$$f(t, SOC, T) = a \cdot t\, b \cdot SOC\, c + d \cdot t \cdot SOC \qquad (4)$$

With:

$$a(T) = a_1 \cdot T^{a_2} + a_3 \qquad (5)$$

$$b(T) = b_1 \cdot T^{b_2} + b_3 \qquad (6)$$

$$c(T) = c_1 \cdot T^{c_2} \qquad (6)$$

$$d(T) = d_1 \cdot T^2 + d_2 \cdot T + d_3 \qquad (7)$$

And the following variables:

Table V: numerical values of the variables from equations 5 till 7.

a_1= -7.007	b_1= 3.459e-14	c_1= 0.003542	d_1= -2.457e-06
a_2= -0.6682	b_2= 7.815	c_2= 1.395	d_2= -0.0001313
a_3= 0.5259	b_3= 0.3124		
d_3= 0.001928			

The result of this equation is pictured in Figure 11, where the lifetime, expressed in years, is estimated for an EOL criterion of 20% capacity loss, in function of Storage SOC from 20% to 100% SOC, and temperature from 25°C to 45°C.

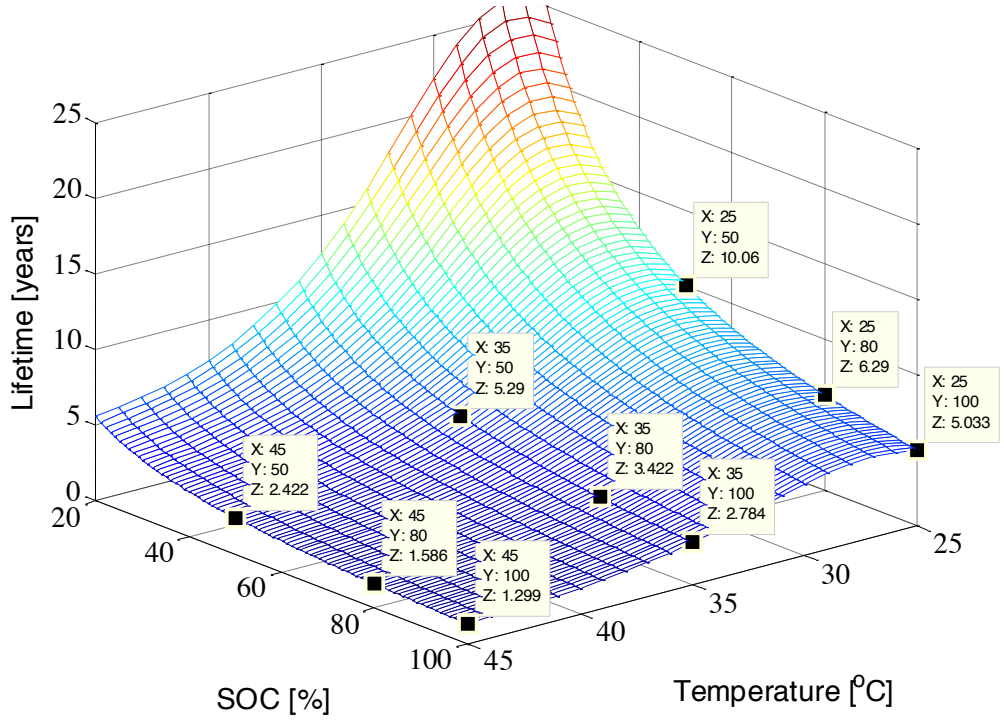

Fig. 11: Calendar lifetime at different conditions (SoC and temperature) until 20% capacity degradation.

The schematic overview of the complete ageing model can be seen in Figure 12.

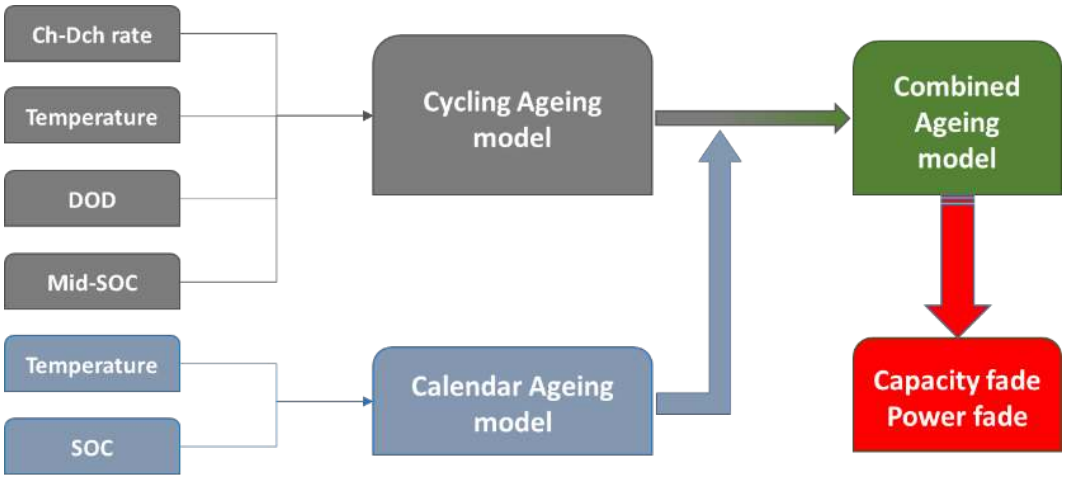

Fig. 12: Schematic overview of the complete ageing model

Thermal modelling and ageing assessment of the thermal parameters

Thermal modelling of the first generation NMC cells

Along with the electrical performance, the thermal characteristic of li-ion batteries is very important topic to study because temperature influences both short-term (capacity, efficiency, self-discharge) and long-term (lifetime) behaviour of lithium-ion batteries. Moreover, the thermal modelling is gaining its importance due to the increased charging and discharging power capabilities of modern batteries and more compact designs of the modern battery packs in order to limit the volumetric energy density of the EV batteries.

Thermal behaviour of the li-ion batteries has been studied in a number of publications and they are usually complex models and they often require coupled electrochemical model to provide accurate information about battery cells temperature evolution at different operating conditions [14-20].
In Batteries 2020 project, a reliable thermal model has been developed to describe the thermal performance of a small stack composed of two li-ion cells during its first life. A simple but very efficient 1D-thermal lumped model has been chosen to limit time and computational resources needed to perform transient simulations. The thermal model was developed in *Matlab/Simulink*® environment in order to make viable the future interaction between the diverse models in the Batteries2020 project.

In the present work, a thermal model of a simple Begin of Life (BOL) first generation (G1) dual cell system (BOL Stack) has been developed and experimentally validated by means of temperature measurements. These measurements are made using K-type thermocouples placed on the symmetry plane between the two cells. An average value of both the temperature measurements will be used as the experimental reference to check it against the model predictions. The expected thermal performance of such a dual system is schematically presented in Figure 13. If the dual system is composed of cells at very different ageing states, a different thermal performance could be expected. This performance should be easily modeled and traced by following the proposed approach and using an adequate test bench. Only the transversal path for the heat diffusion will be considered in this study for simplicity, isolating all the lateral zones of the system.

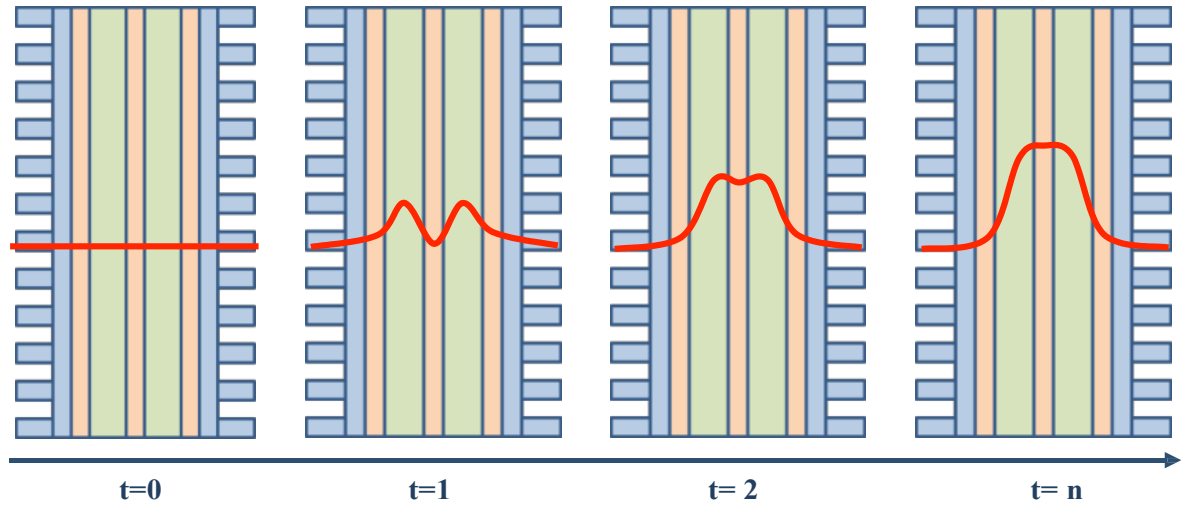

Fig. 13: Thermal transient performance of a dual cell system (green zones represent the cells, orange zones are TIM layers to avoid air spaces and blue zones are some hypothetic heat dissipaters). The red curve represents the evolution of the temperature in time inside the system as different snapshots.

The thermo-electrical parameters that have been used in this case for G1 cells at BOL can be seen in Figure 14 and the used thermo-physical values are provided in Table VI. In order to predict an accurate SOC variation, the sensetivity of the electric capacity with the temperature has been taken into account in the thermal model by means of simple coulomb counting technique.

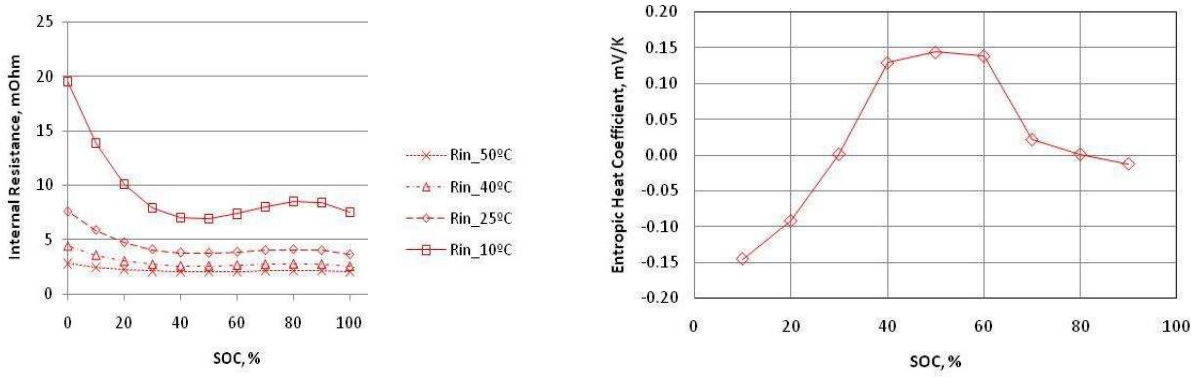

Fig. 14: Thermo-electrical properties of G1 battery cell: internal resistance (left) and the entropic heat coefficient (EHC) (right).

Table VI: Thermo-physical properties of G1 cells.

Parameter	**Value**	**Units**
Mass	0.417	*kg*
Thermal conductivity	1.9	*W/m·K*
Thermal capacity	1254	*J/kg·K*

The developed thermal model was experimentally validated using a custom-made test bench (wind tunnel). In the developed air tunnel, pulse width modulation (*PWM*) was used to control the value of air velocity. The tunnel was calibrated for different values of air velocity (external convective force). The heat dissipation by radiation was neglected.

By maintaining the external forced convective boundary conditions invariable, a complete experimental validation campaign has been performed consisting of 9 tests in the normal operational window (ambient temperatures of 10 °C – 40 °C, C-rates up to 2C, a DOD up to 50% with a middle SOC of 50%) for the G1 cells. External ambient temperature has been modified using a climatic chamber at three different temperature levels: 15 °C, 25 °C and 35 °C. At each ambient temperature level, discharging and charging (DCH/CHA) profiles with different C-rates and different DODs have

been applied to both cells in a parallel electric configuration. The obtained results at 25 °C are presented in Figure 15.

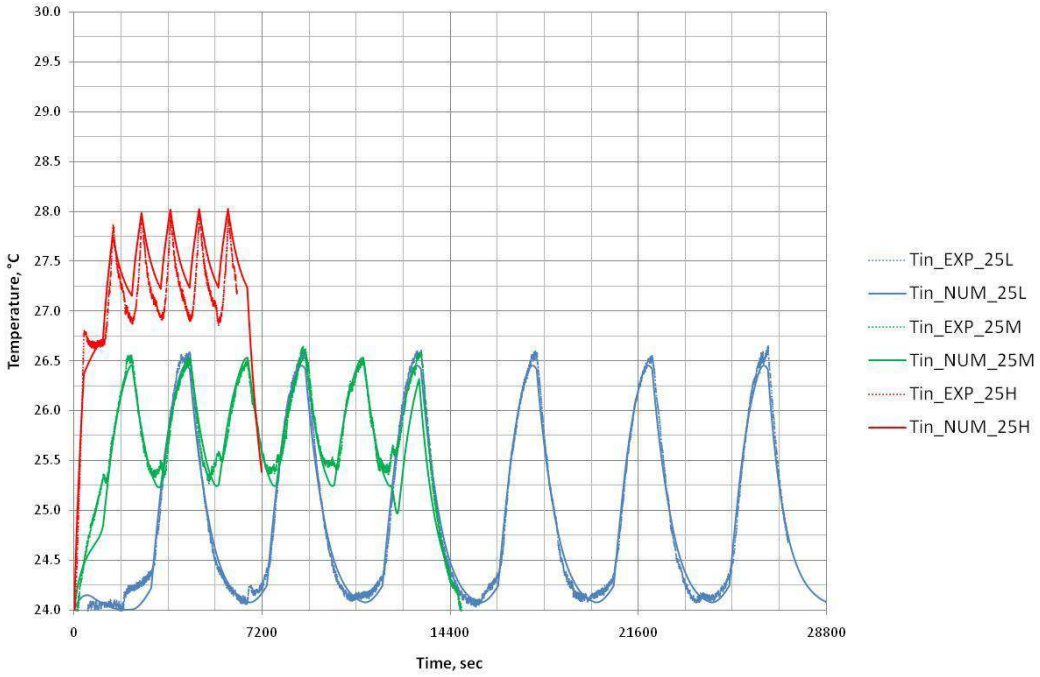

Fig. 15: Comparison between numerical and experimental results for tests at 25°C for L (0.5C current rate with a DOD of 40%), M (1C current rate with 30% DOD) and H (1C charge, 2C discharge current rate with a DOD of 20%) cycles.

An absolute mean time-averaged error of only 0.5% has been achieved in the temperature prediction for very diverse conditions what confirms high accuracy of the developed thermal model. The magnitude error is relatively higher at low temperatures.
The absolute time-averaged error for all 9 tests is presented in Table VII.

Table VII: Absolute time averaged error for 9 tests.

T(°C)	L	M	H
15	0.75%	1.46%	2.85%
25	-0.05%	-0.29%	0.81%
35	-0.38%	-0.42%	0.07%

The evolution of battery cells thermal parameters with battery ageing

In Batteries2020 project, the evolution of the most important thermal parameters for the NMC against grafite G1 cells was investigated in order to determine how battery cell thermal behaviour is changing with battery ageing. The thermal parameters, which were considered for this analysis and which have been determined experimentally, are the internal resistance and the entropic heat coefficient (EHC). These two parameters are considered the most important contributors to the heat generation.

In order to analyze the effect of ageing, which is caused by the different stress factors (i.e. temperature, charging and discharging C-rate, depth-of-discharge (DOD), and middle SOC), nine NMC-based battery cells were aged at the conditions summarized in Table VIII.

Table VIII: Cycle ageing test conditions for nine NMC/C battery cells

Stress factor	I	II	III	IV	V	VI	VII	VIII	IX
C-rate (cha/dcl	C/3 – 1C	C/3 – C/3	C/3 – 1C	C/3 – 2C	C/3 – 1C	C/3 – 1C	C/3 – 1C	C/3 – 1C	C/3 – 1C
T (^{o}C)	25	35	35	35	35	35	35	35	45
DOD (%)	80	80	80	80	80	50	50	50	80
Middle SOC ('	50	50	50	50	65	50	35	50	50
Max SOC (%)	90	90	90	90	90	75	60	60	90
Min SOC (%)	10	10	10	10	40	25	10	40	10
Cell reference	G270	G271	G272	G277	G273	G274	G275	G276	G278

The DC internal resistance of the NMC battery cell is obtained by following the hybrid pulse power characterization (HPPC) test that is presented in Figure 16.

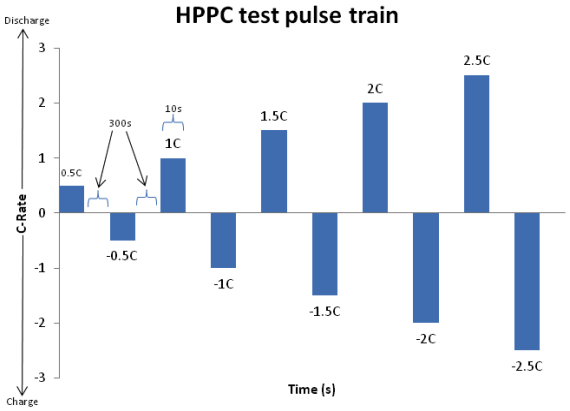

Fig. 16: Applied HPPC pulse train for measuring the DC internal resistance

The obtained results for different test cases are presented in Table IX.

Table IX. DC internal resistance increase for the NMC/C battery cells

Cell	FEC	Temp	R_{in}	Cell	FEC	Temp	R_{in}
G270	1500	25 ^{o}C	8.1 %	G275	1500	35 ^{o}C	4.8 %
G271	1100	35 ^{o}C	24.1 %	G276	1500	35 ^{o}C	46.1 %
G272	1500	35 ^{o}C	82.9 %	G277	1500	35 ^{o}C	117 %
G273	1500	35 ^{o}C	34 %	G278	1300	45^{o}C	163.7 %
G274	1500	35 ^{o}C	16.3 %				

Open circuit potential (OCP) measurements were performed for nine SOC levels, considering a 10% SOC resolution (90:10:10%) during a full discharge of the cell in order to determine the EHC. Thermal cycle, presented in Figure 17, was utilized at different the different SOC levels of the battery cells. The exemplification of the battery cell open circuit voltage response during the thermal cycle is presented in Figure 18.

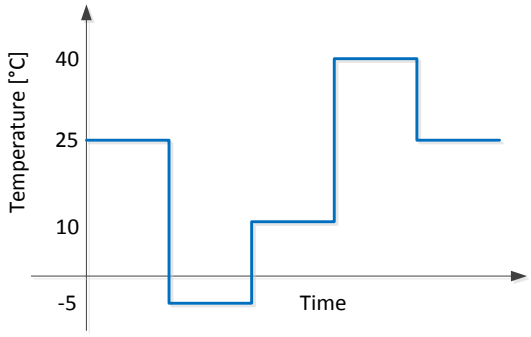

Fig. 17: Applied EHC thermal profile.

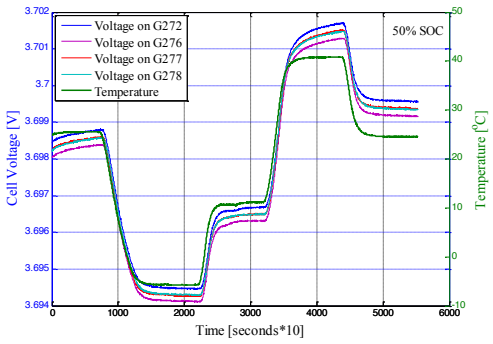

Fig. 18 Battery cells voltage variations at 50% SOC for thermal profile presented in Figure 17.

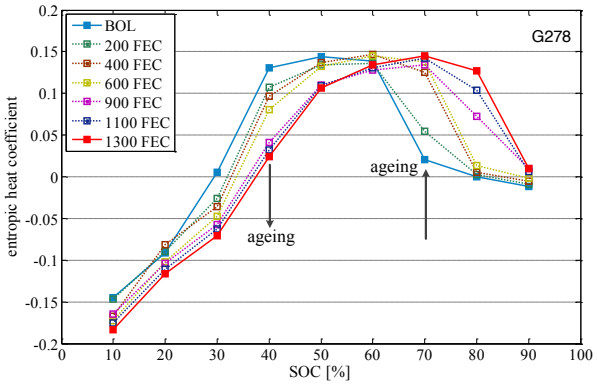

Fig. 19: The EHC values during ageing for cell G278.

The obtained EHC values during ageing for cell with reference G278 are presented in Figure 19.

The obtained results after performing 1500 FEC have shown that studied thermal parameters have shown consistent changes in their values. The DC internal resistance was varying significantly with the battery ageing and is strongly contributing to the irreversible heat generation of the cell.
For the EHC, the most noticeable variations occurred for the most degraded battery cells. The highest values of the EHC shifted from the middle SOC range to the higher SOC values (see Figure 19) during ageing. This EHC trend was consistent with battery ageing.

Second Life Battery Testing Methodology

Application profile definition methodology

Two main applications were considered for the second life battery testing. On the one hand, a Spanish residential household was considered, which is composed of residential loads, a roof-mounted photovoltaic (PV) system and a second life battery energy storage system (herein referred as SLBESS). This application represents a low-demand application, in which low current rates (C-rate) and low depth of discharge (DOD) cycles are mostly recorded. Further details on this residential profile can be found in [21].
On the other hand, a SLBESS is considered in order to mitigate the power variability of a grid-scale PV plant. The unpredictable nature of intermittent renewable energy resources produces significant variability on the power output provided to the grid. Therefore, implementing a SLBESS to reduce such power variability represents a high-demand application, especially in terms of C-rate, DOD and number of cycles-per-year. Further details can be found in [22].
In order to calculate the power demanded from the battery system, the battery pack (BP) sizing optimization methodology described in Figure 20 was followed. After obtaining the optimal sizing of the SLBESS for the two applications, as described in [21], [22], the power demanded to the battery pack during one-year operation is calculated. Considering the G1 cells mentioned before, a series-parallel configuration of the battery system is then defined, which allows assessing the current throughput profile at cell-level.

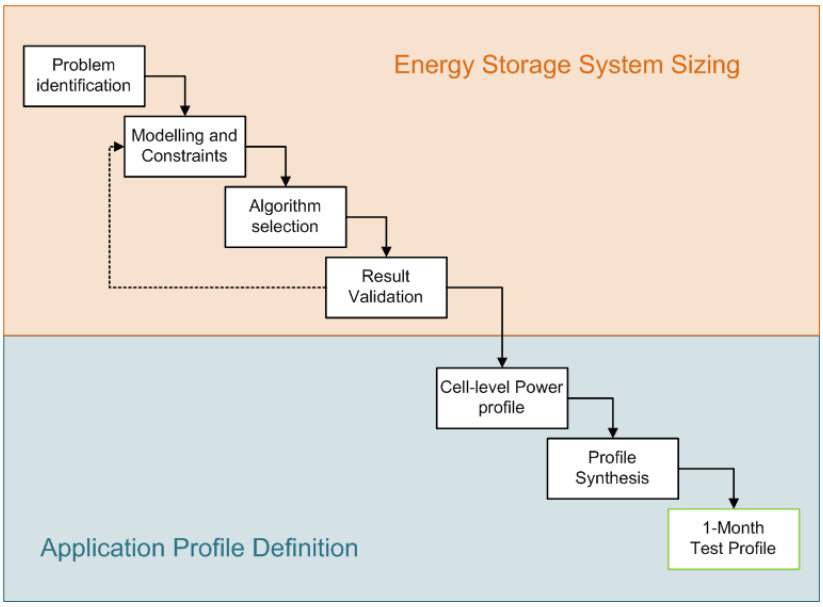

Fig. 20: SLBESS sizing and profile definition methodology.

Figure 21 shows the current demanded to the battery in the two applications described:

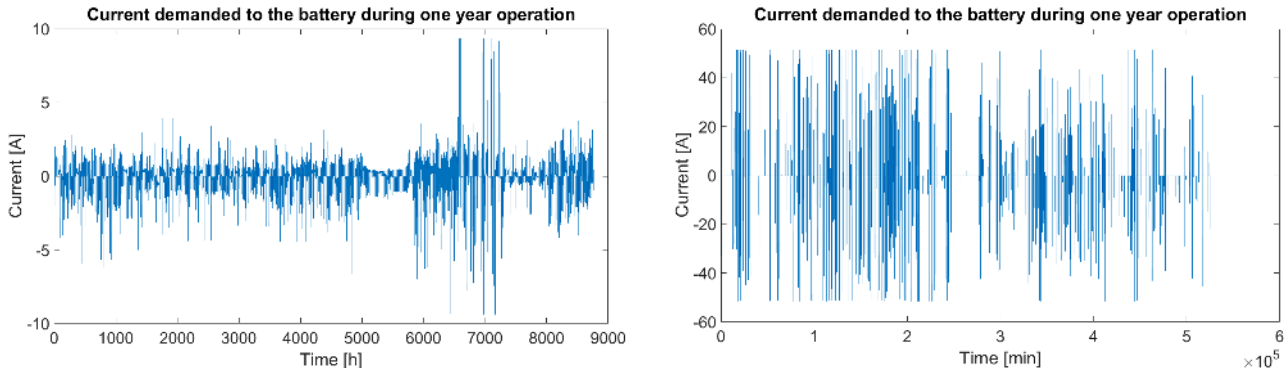

a) b)

Fig. 21: Current demanded from the battery during one-year operation with the optimal SLBESS sizing for a) the residential demand charge management application and b) power smoothing renewable integration application.

Application Profile Synthesis

With the objective of shortening the testing time and obtaining results in the most effective way, the current profiles obtained for each second life application were synthesized. The one-year operation profile of each of the two applications was shortened to an accelerated one-month profile (one per application). Considering the current profiles of the two applications mentioned before, it was observed that most of the time the batteries remain in idle state; this is especially the case of the power smoothing renewable integration application, for which the idle time accounts up to c.a. 95% of the year. The idling operation contributes to the calendar degradation of the battery cells, but it is expected to slow considerably the battery ageing rate. According to the battery ageing behaviour observed in the first life, it is expected that this way of shortening the profiles will also accelerate battery ageing due to an increased ratio of cycling time versus total testing time.

The steps carried out for the synthesis of the application profiles are summarized as follows:

1. **Elimination of the pauses.** The resultant profile after eliminating the pauses in the original application profile is considerably shorter.

2. **Selection of one-month length profile.** In the case when the shortened profile was still longer than the desired one-month profile, the most representative parts of the profile were selected to produce a one-month duration profile.
3. **Introduction of reduced storage time in the one-month profile.** A certain percentage of storage time was introduced intentionally to limit the stress produced by the profile, while enabling the analysis of the effect of coupling storage and cycling periods on battery ageing.

Additionally, in the case of the residential application, the electrical current values were magnified by a factor of four, while each pulse's duration was divided by the same factor of four. This scaling factor contributes to accelerating battery degradation, while keeping the shape of the SoC profile of the tested batteries unchanged.

The one-month duration profile of both residential and power smoothing applications is shown in Figure 22. Compared to the original application profiles, obtained from the sizing approach, the power smoothing application profile comprises the cycling of two-year operation on a single month, whereas the residential application profile covers c.a. 65% of the cycles performed during one-year operation.

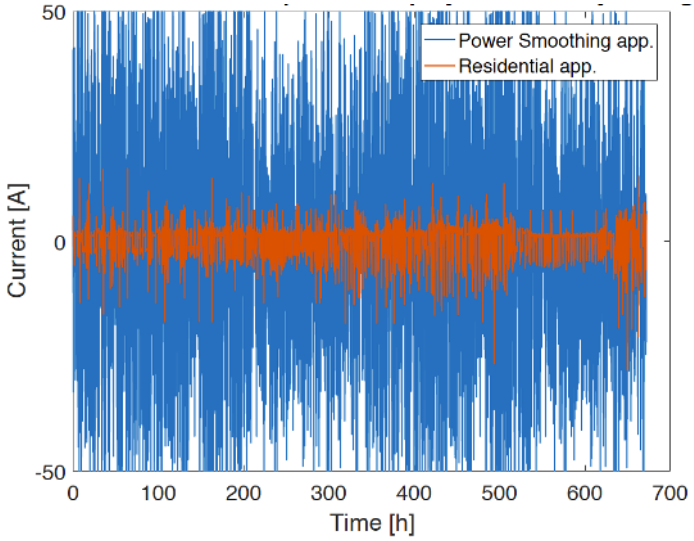

Fig. 22. One-month synthesized current profile of the two applications considered: power smoothing application (blue) and residential application (red).

Second life ageing test plan

Two experimental activities have been considered for the analysis of the performance and degradation behaviour of second life batteries: testing of batteries at cell-level and at stack-level.

It is expected that both first life history – i.e. the stress condition during electric vehicle (EV) use of the batteries – and the selected second life application have a significant effect on second life battery degradation. For this reason, cells with different first life ageing conditions are tested under the two different application profiles: a residential demand response management application and a power smoothing application for a grid-scale PV plant. On the one hand, cells tested in first life with real life EV profiles are used for testing second life batteries at cell level (with the two synthetic application profiles described above). On the other hand, cells tested in first life according to different static ageing conditions (each ageing factor is kept constant over the whole first life testing) are also tested both at cell and at stack level. Stack testing covers only the power smoothing renewable integration application, due to cell and equipment limitations. Each of the considered stacks consists of 3 cells connected in series.

The SOH level of the cells at the end of first life is expected to be a key factor affecting battery performance and degradation behaviour during second life use. For this reason, cells at different SOH levels have been included in the analysis, and SOH heterogeneity has also been taken into account to group the cells at each of the stacks. Cell-to-cell homogeneity/heterogeneity was evaluated in terms of actual capacity, internal resistance and number of cycles performed during first life. Thereby, two

homogeneous stacks and another two heterogeneous stacks were built. The homogeneous stack is composed of cells with similar first life history and similar SOH levels. Contrarily, the heterogeneous stacks were built according to two different criteria:

a) using cells with very different first life history and with very different SOH level, and

b) using two cells coming from the same first life condition and a third one coming from a different first life condition, with a SOH level different from the SOH level of the two other cells (with reduced heterogeneity).

The whole test plan is summarized in Figure 23, where cells coming from different first life conditions are distributed and used for cell-level or stack-level second life testing conditions after being subjected to End of Test (EOT) characterization procedures.

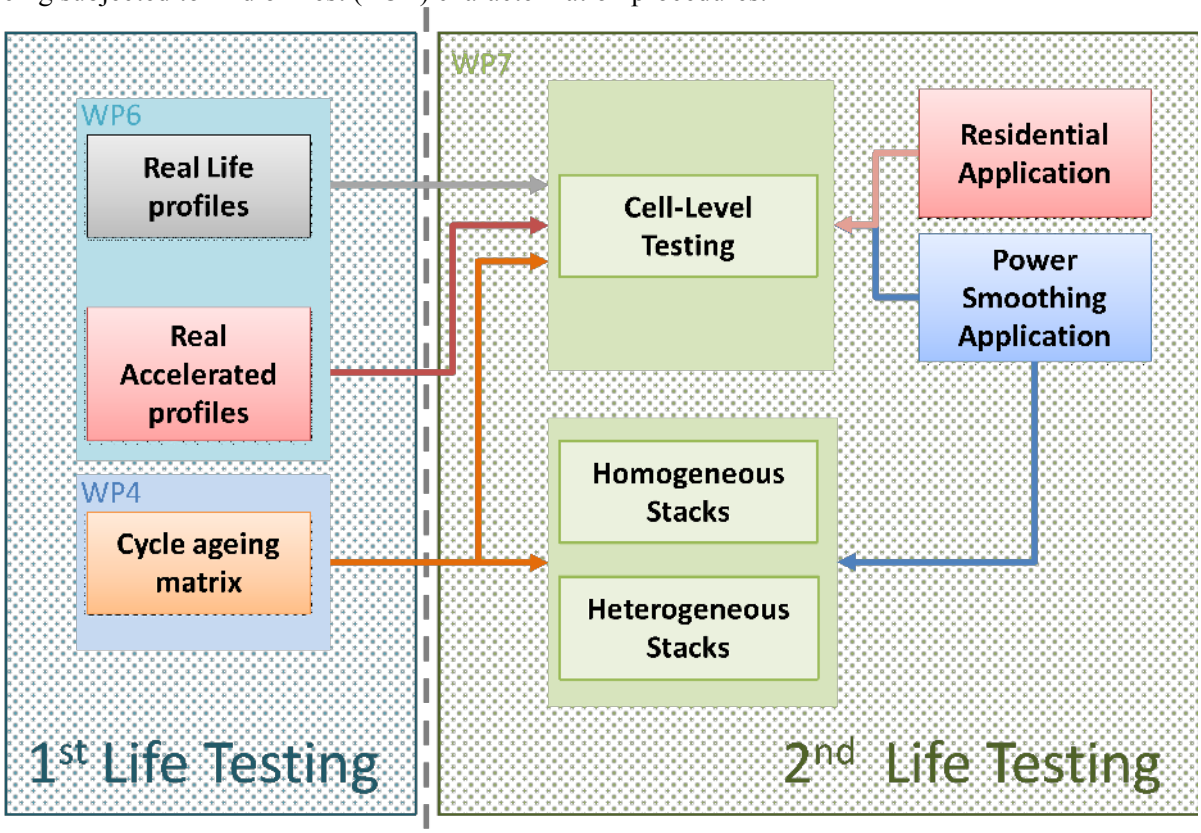

Fig. 23: Block diagram of the transition from the first life testing conditions to the second life testing.

Conclusions

This paper provides a summary of some main outcome of the Batteries 2020 project. A first section is related to the understanding of ageing and degradation mechanisms observed in lithium ion cells. As a conclusion we can say that discharging the cell more deeply before recharging, is not beneficial for the lifetime. Keeping in mind the findings from calendric ageing, long time storage at high SOC levels is not beneficial for the battery ageing. A second section is related to advanced dynamic electrical models developed for the NMC lithium ion batteries. Advanced characterisation procedures in combination with a proper SoC estimation technique results in a well performing electrical ECM model with a good overall accuracy and good representation of the dynamic behaviour of voltage response of the cell. A third section describes the development of a lifetime model. This model is composed of a cycling ageing model and calendar-ageing model and is based on an extensive set of ageing test. A fourth section describes the development of a thermal model and the study of the evolution of the thermal parameters with cell ageing. The DC internal resistance was varying significantly with the battery ageing and is strongly contributing to the irreversible heat generation of the cell. For the EHC, the most noticeable variations occurred for the most degraded battery cells. The

highest values of the EHC shifted from the middle SOC range to the higher SOC values during ageing. Finally, in the fifth section, the methodology designed for second life battery testing was described.

References

[1] M. Daowd, N. Omar, J. Van Mierlo, and P. Van Den Bossche, "An Extended PNGV Battery Model for Electric and Hybrid Vehicles Abbreviations or Glossary :," vol. xx, no. June, 2011.

[2] O. Tremblay, L.-A. Dessaint, and A.-I. Dekkiche, "A Generic Battery Model for the Dynamic Simulation of Hybrid Electric Vehicles," *2007 IEEE Veh. Power Propuls. Conf.*, no. V, pp. 284–289, Sep. 2007.

[3] N. Omar, B. Verbrugge, G. Mulder, P. Van Den Bossche, J. Van Mierlo, and M. Daowd, "Evaluation of performance characteristics of various lithium-ion batteries for use in BEV application."

[4] N. Omar, M. Daowd, P. Van Den Bossche, O. Hegazy, J. Smekens, T. Coosemans, and J. Van Mierlo, "Rechargeable Energy Storage Systems for Plug-in Hybrid Electric Vehicles—Assessment of Electrical Characteristics," *Energies*, vol. 5, no. 12, pp. 2952–2988, Aug. 2012.

[5] M. Einhorn, V. F. Conte, C. Kral, J. Fleig, and R. Permann, "Parameterization of an electrical battery model for dynamic system simulation in electric vehicles," *2010 IEEE Veh. Power Propuls. Conf.*, pp. 1–7, Sep. 2010.

[6] R. a. Jackey, "A Simple, Effective Lead-Acid Battery Modeling Process for Electrical System Component Selection," Apr. 2007.

[7] N. Omar, D. Widanage, M. Abdel Monem, Y. Firouz, O. Hegazy, P. Van den Bossche, T. Coosemans, and J. Van Mierlo, "Optimization of an advanced battery model parameter minimization tool and development of a novel electrical model for lithium-ion batteries," *Int. Trans. Electr. Energy Syst.*, p. n/a–n/a, Oct. 2013.

[8] A. Nikolian, J. De Hoog, K. Fleurbay, J. Timmermans, P. Van De Bossche, and J. Van Mierlo, "Classification of Electric modelling and Characterization methods of Lithium-ion Batteries for Vehicle Applications," *Eur. Electr. Veh. Congr.*, no. December, pp. 1–15, 2014.

[9] A. Nikolian, Y. Firouz, R. Gopalakrishnan, J.-M. Timmermans, N. Omar, P. van den Bossche, and J. van Mierlo, "Lithium Ion Batteries—Development of Advanced Electrical Equivalent Circuit Models for Nickel Manganese Cobalt Lithium-Ion," *Energies*, vol. 9, no. 5, p. 360, 2016.

[10] IEC, "IEC 62660-1: Secondary lithium-ion cells for the propulsion of electric road vehicles - Part 1: Performance testing," 2010.

[11] ISO, "ISO 12405-1:2011 - Electrically propelled road vehicles -- Test specification for lithium-ion traction battery packs and systems -- Part 1: High-power applications."

[12] ISO, "ISO 12405-2: Electrically propelled road vehicles — Test specification for lithium-ion traction battery packs and systems — Part 2 : High energy application," no. 20, 2009.

[13] IEC, "IEC 61982-2: Secondary batteries for the propulsion of electric road vehicles - Part 2: Dynamic discharge performance test and dynamic endurance test," 2002.

[14] Bernardi D., Pawlikowski E., Newman J., 1985, A general energy balance for battery systems, J. Electrochem. Soc., 132, 5-12.

[15] Doyle M., Fuller T., Newman J., 1993, Modeling of galvanostatic charge and discharge of the lithium/polymer/insertion cell, J. Electrochem. Soc., 140, 1526-1533.

[16] Chen Y., Evans J., 1993, Heat transfer phenomena in lithium polymer-electrolyte batteries for electric vehicle application, J. Electrochem. Soc., 140, 1833-1838.

[17] Newman J., Tiedemann W., 1995, Temperature rise in a battery module with constant heat generation, J. Electrochem. Soc., 142, 1054-1057.

[18] Pals C., Newman J., 1995, Thermal modelling of the lithium/polymer battery, J. Electrochem. Soc., 142, 3274-3281.

[19] Doyle M., Newman J., Gozdz A., Tarascon J.M., 1996, Comparison of modeling predictions with experimental data from plastic lithium ion cells, J. Electrochem. Soc., 143, 1890-1903.

[20] Thomas K., Newman J., 2003, Thermal modelling of porous insertion electrodes, J. Electrochem. Soc., 150, A176-A192.

[21] A. Saez-de-Ibarra, E. Martinez-Laserna, C. Koch-Ciobotaru, P. Rodriguez, D.-I. Stroe, and M. Swierczynski, "Second Life Battery Energy Storage System for Residential Demand Response Service," in IEEE International Conference on Industrial Technology (ICIT), 2015.

[22] C. Koch-Ciobotaru, A. Saez-de-Ibarra, E. Martinez-Laserna, D.-I. Stroe, M. Swierczynski, and P. Rodriguez, "Second life battery energy storage system for enhancing renewable energy grid integration," Energy Conversion Congress and Exposition (ECCE), 2015 IEEE. pp. 78–84, 2015.